ISSN 0036-0244, Russian Journal of Physical Chemistry A, 2021, Vol. 95, No. 6, pp. 1165–1168. © Pleiades Publishing, Ltd., 2021.
Russian Text © The Author(s), 2021, published in Zhurnal Fizicheskoi Khimii, 2021, Vol. 95, No. 6, pp. 903–907.

STRUCTURE OF MATTER AND QUANTUM CHEMISTRY

Diffusion of Strontium in the Intergranular Boundaries of $La_{2-x}Sr_xCuO_4$

A. A. Bykov[a,*], D. M. Gokhfeld[b], K. Yu. Terent'ev[b], M. N. Volochaev[b], and M. I. Petrov[b]

[a] *Petersburg Institute of Nuclear Physics, National Research Center Kurchatov Institute, Gatchina, 188300 Russia*

[b] *Kirensky Institute of Physics, Siberian Branch, Russian Academy of Sciences, Krasnoyarsk, 660036 Russia*

**e-mail: redi87@bk.ru*

Received May 15, 2019; revised October 21, 2020; accepted October 21, 2020

Abstract—Energy dispersive X-ray spectroscopy and scanning electron microscopy are used to study La_2CuO_4–$La_{1.56}Sr_{0.44}CuO_4$ composites with different annealing times. Maps of the strontium distribution for such systems are calculated and compared to experimental data obtained for the area of contact between two dissimilar granules. The coefficient of lattice diffusion of strontium is found. At the areas of contact between La_2CuO_4 and $La_{1.56}Sr_{0.44}CuO_4$ granules, the strontium concentration corresponds to superconducting phase $La_{2-x}Sr_xCuO_4$ with $x = 0.05$–0.25. The technological parameters of synthesis affect the size and number of superconducting and normal regions. Prolonged annealing lowers the gradient of the strontium concentration, which halts the increase in the size of the superconducting regions. This saturation confirms the diffusion front model.

Keywords: composites, superconductivity, diffusion, grain boundaries, diffusion front, LSCO ($La_{1.56}Sr_{0.44}CuO_4$)

DOI: 10.1134/S0036024421060066

INTRODUCTION

The uniform diffusion of precursors and establishing the optimum stoichiometry in a system are usually desirable in solid phase synthesis. In some cases, however, the goal of synthesis could be a nonuniform final distribution of elements. For example, a material with a melting temperature lower than that of a superconducting matrix is used during synthesis to create pinning centers that penetrate a superconducting matrix [1]. The interphase diffusion of elements can result in the formation of new phases in composite materials. In [2], a superconducting layer with an increased critical temperature emerged at the interface between two non-superconducting La_2CuO_4 and $La_{1.56}Sr_{0.44}CuO_4$ films. In [3, 4], composite materials were made from a mixture of non-superconducting La_2CuO_4 (LCO) and $La_{1.56}Sr_{0.44}CuO_4$ ceramics with different annealing times. The resulting materials displayed superconducting behavior corresponding to $La_{2-x}Sr_xCuO_4$ (LSCO), where $x \approx 0.15$ [5]. The fraction of the superconducting phase grew along with annealing time. As suggested in [3], superconducting regions arise because of the diffusion of Sr from granules with an excess of it to granules with a Sr deficiency.

Diffusion and depth profiles of an element in superconducting films were studied earlier via ion backscattering [6] and scanning electron microscopy (SEM) [7]. Unlike films, diffusion in ceramic samples depends strongly on the development of the boundaries along which diffusion takes place, which complicates their study. The aim of this work was direct observation of the lattice diffusion of strontium between grains of La_2CuO_4 and $La_{1.56}Sr_{0.44}CuO_4$.

EXPERIMENTAL

La_2CuO_4 and $La_{1.56}Sr_{0.44}CuO_4$ ceramics were manufactured via solid-phase synthesis [3]. A mixture of non-superconducting La_2CuO_4 and $La_{1.56}Sr_{0.44}CuO_4$ granules with a mass ratio of 0.66 : 0.34, respectively, was annealed for different times t_a (60 to 600 min) at a temperature of 910°C. The proportion of the composite's components corresponds to the nominal formula of optimum superconducting phase $La_{1.85}Sr_{0.15}CuO_4$. In contrast to synthesis with the sintering temperature raised for different samples [8], annealing at a temperature below melting allows us to restore the optimum oxygen concentration.

Samples annealed for $t_a = 60$, 200, and 600 min were investigated via SEM on a Hitachi TM 3000 unit. Macroscopic characterization and micrographs of the considered samples were presented in [3]. Elemental analysis was performed using a Bruker XFlash 6T/60 energy dispersive spectrometer (EDS). A cross section of the diffusion region suitable for study was prepared using an FB2100 focused ion beam setup (Hitachi, Japan). Liquid gallium was used as the ion source, and the accelerating voltage was 10–40 kV. Before each experiment, the samples were polished on a grinding

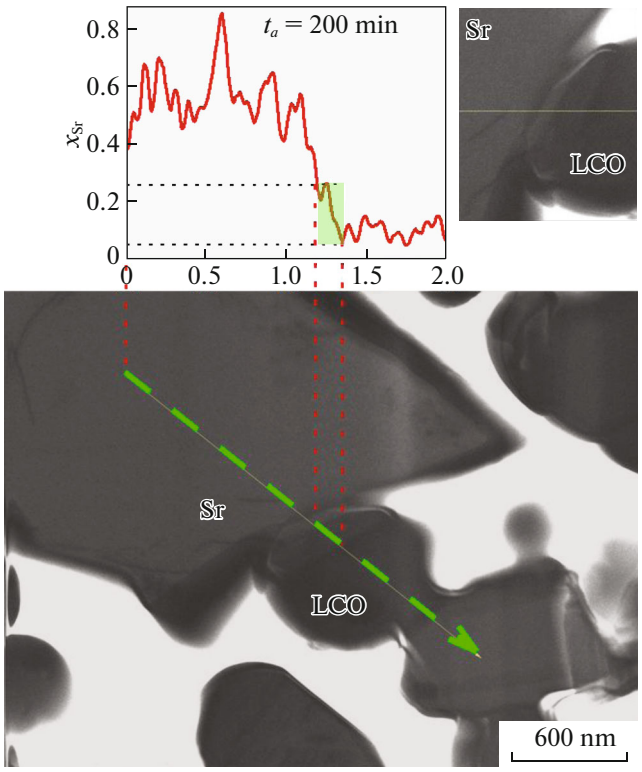

Fig. 1. Micrograph of a sample annealed for t_a = 200 min and Sr distribution.

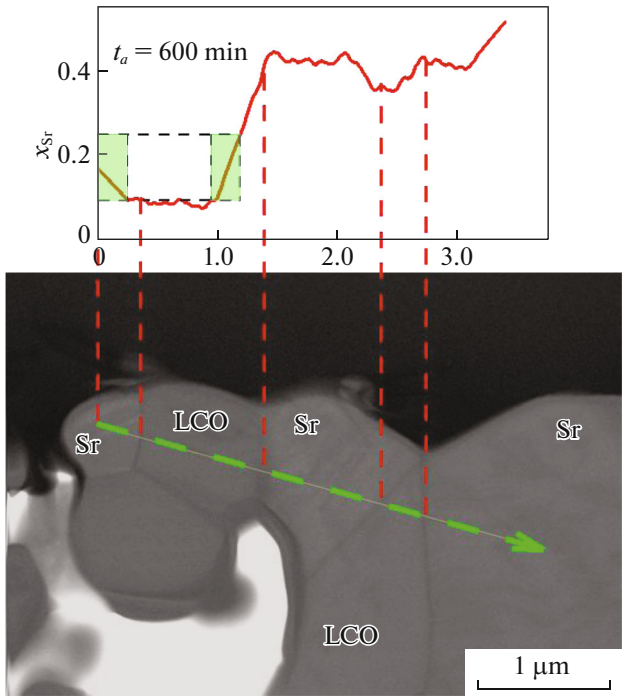

Fig. 2. Micrograph of a sample annealed for t_a = 600 min and Sr distribution.

table using a paste with abrasive particles ~1 μm in size. A thin plate (lamella) was cut from the depth of the sample using a focused ion beam. A micromanipulator with an attached needle was brought to the edge of the lamella until they touched. The needle and lamella were soldered to each other with a beam of tungsten ions. The bridge on which the lamella was held was then cut off with a gallium beam, and the lamella was removed from the sample. The cut went through the granules of the composite and along the places of their fusion. The resulting lamella was transferred with a micromanipulator and soldered with a tungsten beam onto a holder for SEM and EDX. This way of preparing the samples allowed us to study the area of contact between granules from their depths, eliminating the surface effects of diffusion. As in [6], no other ways of studying the division between boundary and lattice diffusion were used. Since the electron beam in SEM is fairly well focused, concentrations can be measured with good spatial resolution. A general view of such a flat cut is shown in Figs. 1–3. The direction of scanning is indicated by the arrow.

RESULTS AND DISCUSSION

Figures 1, 2, and 3a show a general view of the lamellas obtained for samples with t_a = 200, 600, and 60 min. Here and below, granules of composition $La_{1.56}Sr_{0.44}CuO_4$ are labeled Sr; those of composition La_2CuO_4, as LCO.

The insets in Figs. 1–3 show the atomic fractions of Sr at transitions through intergranular boundaries along the normal to the surface of granule contact (the normals are indicated by arrows in the figures). The scales of the abscissa axes of all insets are relative to one another. The range of strontium concentrations corresponding to those of superconductor LSCO (77 to 386 kg/m^3 [5]) is marked with a green rectangle.

The dielectric characteristics of the material changed along with the strontium concentration [5]. Areas with altered strontium concentrations become visible in SEM images due to differences between the drainage of electric charge accumulated via electron beam bombardment. The boundaries between the granules in the micrographs are clearly visible as dark stripes. The correspondence between the grain boundaries and jumps in the Sr concentration on the distribution is shown by red dashed lines.

NUMERICAL CALCULATIONS

Two types of diffusion can be distinguished in ceramic high-temperature superconductors [9]: fast (through pores, twinning boundaries, domains, and granule boundaries) and slow (through the crystal lattice inside the granules). When considering diffusion along the normal to the intergranular boundary, boundary diffusion can be ignored in calculations.

Lattice diffusion in crystals with no allowance for boundaries and defects is described by the parabolic partial differential equation

$$\frac{\partial\varphi(\mathbf{r},t_a)}{\partial t_a} = \nabla\left[D(\varphi,\mathbf{r})\nabla\varphi(\mathbf{r},t_a)\right],$$

where $\mathbf{r}$ is the radius vector in whose direction diffusion occurs, $\varphi(\mathbf{r},t_a)$ is the dopant concentration, and $D(\varphi,\mathbf{r})$ is the coefficient of diffusion. The numerical method of finite elements was used to solve this equation. In contrast to an analytical solution, it allows us to solve diffusion problems for such complex geometries as granular systems. The geometric area in which a solution is sought, is divided into a network of individual elements. In each element of the network, the Sr concentration is approximated by a fourth-order polynomial. The behavior of the entire system is determined by a system of diffusion equations for each element of the network. The boundary conditions were specified as Dirichlet conditions, with the concentration equal to zero at a boundary. Dependence D_{Sr} on concentration and temperature for the LSCO composition was taken from [10]. In this work, we used the MatLab software package for technical calculations.

The rectangle in Fig. 3a shows the region for which diffusion calculations were made. The same region of the micrograph with the superimposed abscissa axis is shown in the inset in Fig. 3b, which presents the calculated map of strontium concentrations for the geometry of the studied lamella and annealing time t_a = 60 min. Figure 3c shows the calculated and experimental dependences of the atomic fraction of strontium on the position along the line of contact between the granules. The calculations were made for a geometry in which the diffusion front did not have time to propagate and be distorted by the geometry of the granules, which happens at brief annealing times.

The calculated curve with $D = 4.84 \times 10^{-17}$ m^2/s does not reproduce the segment of the sharp change in the Sr concentration that is present in the experimental distribution (Fig. 3c). This value of the diffusion coefficient was obtained via layer-by-layer radiometric analysis [10]. The discrepancy between the calculations and the experimental distribution is due to value D being obtained for polycrystalline samples in which diffusion dominated along the grain boundaries [10]. In our case, however, the main role was played by lattice diffusion, which was considerably less than the boundary form. The calculated curve describes the sharp inflection of the experimental distribution when using $D = 5 \times 10^{-18}$ m^2/s (i.e., an order of magnitude less than the one obtained in [10]).

The view of the superconducting front on the calculated scattering map (Fig. 3b) is similar to an asymmetric lens protruding toward the La_2CuO_4 granule, which corresponds to the shape of the diffusion front obtained from the experimental micrograph in the inset. The scale of the circulation of the superconducting current (i.e., the average size of the superconducting islands) was estimated in [3] from the magnetization hysteresis loops, using the extended critical state model [11]. It was shown that the size of superconducting islands is virtually independent of annealing time. It was suggested that the superconducting region is created in the form of a diffusion front. The emergence of a diffusion front is shown schematically in

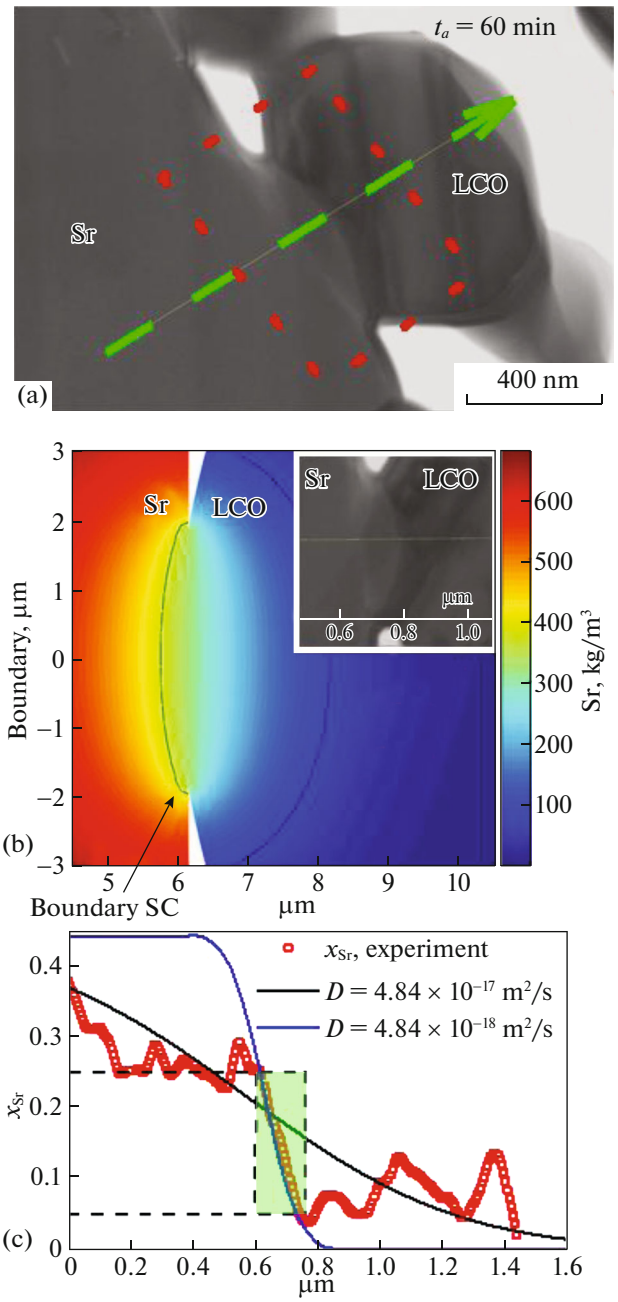

Fig. 3. (a) Micrograph of the contact point of dissimilar La_2CuO_4 granules and $La_{1.56}Sr_{0.44}CuO_4$ for t_a = 60 min. (b) Calculated map of strontium concentration at the contact point of non-superconducting granules. The superconducting region is bounded by black curves. (c) Experimental and calculated values of the atomic fraction of Sr.

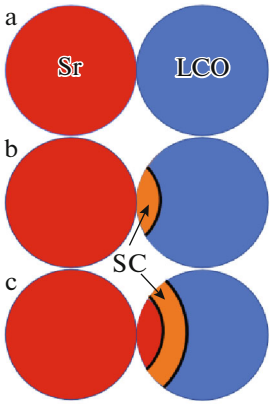

Fig. 4. Diagram of the emergence of a diffusion front. See text for notation.

Fig. 4. Figure 4a shows contact between dissimilar granules. Upon annealing, a region of Sr concentrations appears at the point of contact that corresponds to the superconducting state (SC). The superconducting region is in the form of an asymmetric lens (Fig. 4b). Upon further annealing, Sr diffuses into the depth of the LCO granule (Fig. 4c). In the region of contact between granules, however, the Sr concentration rises above the superconducting one. A diffusion front appears; i.e., a region of Sr concentrations corresponding to that of a superconductor. Behind it, the Sr concentration is excessively high; in front of it, the concentration is excessively low.

The asymmetry of the superconducting region, and the general emergence of one diffusion front rather than two propagating in opposite directions, is a result of the asymmetry of the range of superconducting concentrations (77 to 386 kg/m^3), relative to the average concentration between La_2CuO_4 and $La_{1.56}Sr_{0.44}CuO_4$ (339.5 kg/m^3). In our calculations, the diffusion front was pronounced when one granule was larger than the other. In [3], saturation was established from the change in the superconducting properties of the system depending on the duration of sintering, as was also confirmed by numerical calculations. Saturation occurred due to a drop in the gradient of the strontium concentration, and hence the rate of diffusion.

The graph in Fig. 3c shows that the Sr concentration changed abruptly upon crossing the intergranular boundary. We therefore directly observe the boundary of the diffusion front during the sintering of dissimilar granules. In Fig. 3c, the green rectangle shows the region corresponding to the concentrations of the LSCO superconductor (i.e., the region of existence of the diffusion front, established experimentally). For the sample annealed for 60 min, the calculated width of the diffusion front (≈1.5 μm) coincides with the experimental width. For long annealing times, the calculated values of the diffusion front width greatly exceed the experimental ones. This difference is explained by a drop in the Sr concentration at the point of contact in a real sample as a result of surface diffusion, which was not considered in our calculations.

Energy dispersive X-ray spectroscopy and scanning electron microscopy were thus used for the first time to study the lattice diffusion of strontium and the formation of superconducting phase La_2CuO_4–$La_{1.56}Sr_{0.44}CuO_4$ on single intergranular boundaries.

CONCLUSIONS

1. The diffusion of strontium produces superconducting phase $La_{1.85}Sr_{0.15}CuO_4$ in the region of contact between dissimilar non-superconducting grains of composite La_2CuO_4–$La_{1.56}Sr_{0.44}CuO_4$.

2. The estimated value of the coefficient of the lattice diffusion of strontium is $D = 5 \times 10^{-18}$ m^2/s.

3. Prolonged annealing lowers the gradient of strontium concentration, which halts the growth of the size of the superconducting regions. The stabilization of the dimensions of the superconducting regions confirms our model of the diffusion front.

ACKNOWLEDGMENTS

Our measurements were made on equipment of the Krasnoyarsk Regional Resource Center of the Kirensky Institute of Physics.

FUNDING

This work was supported by the Russian Science Foundation, project no. 17-72-10067.

REFERENCES

1. Y. Yoshida, S. Miura, Y. Tsuchiya, Y. Ichino, S. Awaji, K. Matsumoto, and A. Ichinose, Supercond. Sci. Technol. **30** (10), 104002 (2017).
2. G. Logvenov, A. Gozar, and I. Bozovic, Science (Washington, DC, U. S.) **326** (5953), 699 (2009).
3. A. A. Bykov, K. Y. Terent'ev, D. M. Gokhfeld, et al., J. Supercond. Nov. Magn. **31**, 3867 (2018).
4. A. A. Bykov et al., J. Supercond. Nov. Magn. **32**, 3797 (2019).
5. N. Plakida, *High-Temperature Cuprate Superconductors,* Vol. 166 of *Springer Ser. in Solid-State Science* (Springer, Berlin, Heidelberg, 2010).
6. L. P. Chernenko, A. P. Kobzev, D. A. Korneev, and D. M. Shirokov, Mikrochim. Acta **114–115**, 239 (1994).
7. B. J. Shaw, J. Appl. Phys. **47**, 2143 (1976).
8. N. S. Pavan Kumar, N. Devendra Kumar, R. P. Missak Swarup, et al., Phys. C (Amsterdam, Neth.) **487**, 72 (2013).
9. T. D. Dzhafrov, Phys. Status Solidi **158**, 335 (1996).
10. M. V. Slinkina, L. I. Volosnceva, A. A. Fotiev, and V. R. Hrustov, Supercond. Phys., Chem. Tech. **5**, 706 (1992).
11. D. M. Gokhfeld, Tech. Phys. Lett. **45**, 1 (2019).